Catal Lett (2009) 131:250–257
DOI 10.1007/s10562-009-0057-1

Propane Oxidative Dehydrogenation Over Ln–Mg–Al–O Catalysts (Ln = Ce, Sm, Dy, Yb)

Gheorghiţa Mitran · Adriana Urda · Nathalie Tanchoux · François Fajula · Ioan-Cezar Marcu

Received: 10 March 2009 / Accepted: 4 June 2009 / Published online: 23 June 2009

Abstract Ln–Mg–Al mixed oxide catalysts (Ln = Ce, Sm, Dy, Yb) were prepared from layered double hydroxide precursors, characterized using XRD, N_2 adsorption, TG-DTG, EDX, H_2-TPR and CO_2-TPD techniques and tested in the oxidative dehydrogenation of propane in the temperature range 450–600 °C. For all the catalysts the conversion increases with increasing the reaction temperature while the propene selectivity decreases to the benefit of carbon oxides for Ce-based system and of cracking products for the others. The best yields in propene were obtained with Dy- and Sm–Mg–Al–O catalysts. No correlation between the reducibility of the rare-earth cation and the catalytic performances was observed. A linear correlation between the catalyst basicity and the propene selectivity was evidenced.

Keywords Oxidative dehydrogenation · Propane · Rare-earth oxides · Layered double hydroxides

1 Introduction

The oxidative dehydrogenation of propane to propene is one of the potentially important catalytic processes for the effective utilization of light alkanes and has been thoroughly studied in recent times [1–14], propene being an important raw material for the production of polypropylene, acrylonitrile, acrolein and acrylic acid. In spite of this high number of studies there is no up to now a sufficiently active and selective catalyst for the oxidative dehydrogenation of propane to propene that could be used at industrial scale. Thus, the development of a catalyst with a sufficiently high activity and selectivity is highly desirable.

Heterogeneous catalysts for this reaction typically contain vanadium and molybdenum as the critical elements [1–9]. Among other oxide systems, those containing rare-earth oxides are also reported as active and selective [14–16].

It has been shown that γ-Al_2O_3-supported rare-earth oxides (Y, Dy, Tb, Yb, Ce, Tm, Ho and Pr) are reactive in propane oxidative dehydrogenation, but propene selectivities were relatively low, namely under 40% [14]. Taking into consideration the electron-donating character of the olefinic species, it was of interest to investigate whether the propene selectivity could be enhanced by increasing the catalyst basicity. For this reason we prepared Mg–Al mixed oxide-supported rare-earth oxides from layered double hydroxide (LDH) precursors and we studied their catalytic properties in the oxidative dehydrogenation of propane. The obtained results are presented in this paper.

2 Experimental

2.1 Catalysts Preparation

Ln–Mg–Al–O (Ln = Ce, Sm, Dy, Yb) samples were prepared by coprecipitation of mixed metal nitrate solutions with an aqueous solution of NaOH (2 M) at a constant pH of 10. Thus, an aqueous solution of $Mg(NO_3)_2{\cdot}6H_2O$ and

G. Mitran · A. Urda · I.-C. Marcu (✉)
Department of Chemical Technology and Catalysis, Faculty of Chemistry, University of Bucharest, 4-12, Blv. Regina Elisabeta, 030018 Bucharest, Romania
e-mail: marcu.ioan@unibuc.ro; ioancezar_marcu@yahoo.com

N. Tanchoux · F. Fajula
Institut Charles Gerhardt, UMR 5253 CNRS/ENSCM/UM2/UM1, Matériaux Avancés pour la Catalyse et la Santé (MACS), Ecole Nationale Supérieure de Chimie, 8, rue de l'Ecole Normale, 34296 Montpellier Cedex 5, France

$Al(NO_3)_3{\cdot}9H_2O$ was contacted with the basic solution by dropwise addition of both solutions into a well-stirred beaker containing 200 cm^3 of rare-earth Ln nitrate solution at room temperature. Ln content, as atomic percent with respect to the cationic species, was equal to 5 and the Mg/Al atomic ratio was kept at 3 for all preparations. The addition of the alkaline solution and pH were controlled by pH-STAT Titrino (Metrohm). The precipitates formed were aged in their mother liquor overnight at 80 °C under stirring, separated by centrifugation, washed with deionized water until a pH of 7 and dried at 80 °C overnight. Dried samples were calcined in air at 750 °C during 8 h in order to form the corresponding mixed metal oxides which were used as catalysts.

2.2 Catalysts Characterization

Powder X-Ray diffraction (XRD) spectra were obtained using a Siemens D5000 Diffractometer and monochromatic Cu-Kα radiation. They were recorded with 0.02° (2θ) steps over the 3°–70° ← angular range with 1 s counting time per step.

The chemical composition of the samples was determined by EDX microprobe on a Cambridge Stereoscan 260 apparatus.

The textural characterization was achieved using conventional nitrogen adsorption/desorption method, with a Micromeritics ASAP 2010 automatic analyzer. Prior to nitrogen adsorption, the samples were outgassed for 8 h at 523 K.

The thermal analysis (TG and DTG) was carried out using a Netzsch TG 209 device, in the following conditions: linear heating rate 10 °C min^{-1} from room temperature to 900 °C, dynamic air atmosphere, Al_2O_3 crucible, sample weight approximately 20 mg.

Temperature-programmed desorption (TPD) of CO_2 was carried out using a Micromeritics Autochem model 2910 instrument. Fresh calcined samples (100 mg) were pretreated in air at 550 °C before adsorption of the probe molecule at 100 °C. During desorption, the sample was heated in a helium flow (30 mL min^{-1}) at a ramp of 10 °C min^{-1}. The amount of the probe molecule desorbed from the sample was estimated from the area under the peak after taking the thermal conductivity detector response into consideration.

Hydrogen temperature-programmed reduction (H_2-TPR) studies were carried out using a Micromeritics Autochem model 2910 instrument. Fresh calcined samples (100 mg), placed in a U-shaped quartz reactor, were pretreated in air at 750 °C before reduction. After cooling down to room temperature and introducing the reduction gas of 3% H_2/Ar, the sample was heated at a rate of 10 °C min^{-1} from room temperature to 800 °C. The hydrogen consumption was estimated from the area under the peak after taking the thermal conductivity detector response into consideration. Calibration of TCD signal has been done with an Ag_2O standard (Merck, reagent grade).

Characterization of the samples has been performed before and, for some of them, after the catalytic test.

2.3 Catalytic Testing

The catalytic oxidative dehydrogenation of propane was carried out in a fixed bed quartz tube down-flow reactor operated at atmospheric pressure. The internal diameter of the reactor tube was 15 mm. The catalyst was supported by quartz wool. The axial temperature profile was measured using an electronic thermometer placed in a thermowell centered in the catalyst bed. Quartz chips were used to fill the dead volumes before and after the catalyst bed to minimize potential gas-phase reactions at higher reaction temperatures. The gas mixture consisting of propane and air was fed into the reactor at a volume hourly space velocity (VHSV) in the range of 3,000–12,000 h^{-1}. The reaction temperature was varied between 450 and 600 °C, the propane-to-oxygen molar ratio, between 1 and 4, and the catalyst bed volume was always kept to 1 cm^3. In a typical reaction run, the reactor was heated to the desired temperature in the flow of reactants. The system was allowed to stabilize for about 1 h at the reaction temperature before the first product analysis was made. Each run was carried out over a period of 2–3 h. The reaction products were analyzed in a Clarus 500 Gas-Chromatograph equipped with a thermal conductivity detector (TCD) using an alumina column and a flame ionization detector (FID) using a CTR I column.

Propene, CO, CO_2 and cracking products (methane and ethylene) were the major products formed under the reaction conditions. Conversion of propane and product selectivities were expressed as mol% on a carbon atom basis. The carbon balance was in all runs higher than 95%.

3 Results and Discussion

3.1 Catalysts Characterization

The XRD patterns of the prepared precursors and final catalysts are displayed in Figs. 1 and 2, respectively. Poorly crystallized layered hydrotalcite-type structures (JCPDS 37-0630), as generally observed for multicationic LDH, were detected on all dried precipitated samples labeled LnMgAl-LDH. The interlayer distance 003 equal to ca. 8 Å, was consistent with the presence of nitrates as interlayered [17]. Some of the samples, as Ce-, Sm- and DyMgAl-LDH, displayed lines corresponding to poorly crystallized CeO_2 (JCPDS 75-0076) $Sm(OH)_3$ (JCPDS 83-2036) and Dy_2O_3

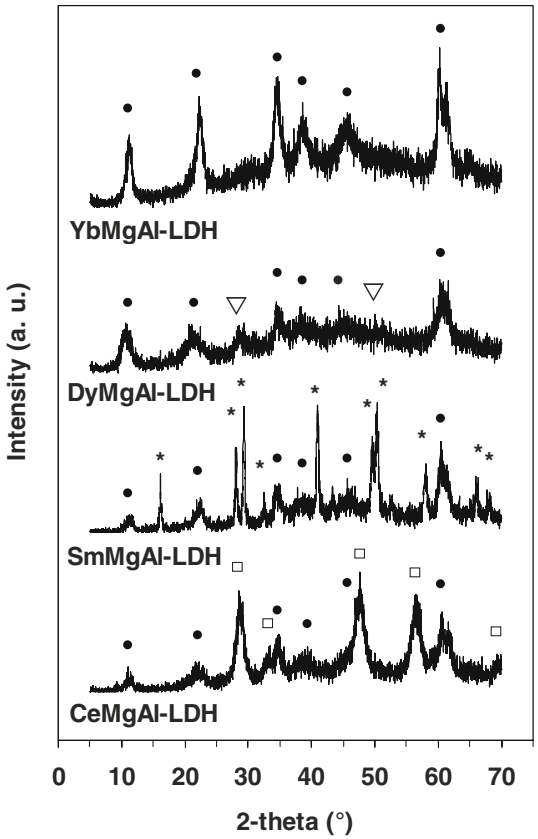

Fig. 1 XRD patterns of the LDH precursors (●: layered hydrotalcite-type structure, □: CeO_2, *: $Sm(OH)_3$, ∇: Dy_2O_3)

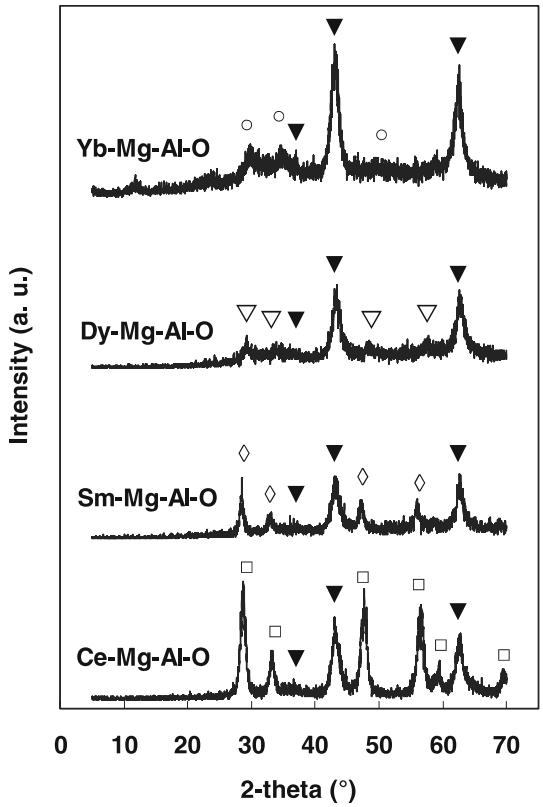

Fig. 2 XRD patterns of the final mixed-oxide catalysts after calcination at 750 °C (▼: MgAlO mixed oxide phase, □: CeO_2, ◇: Sm_2O_3, ∇: Dy_2O_3, ○: Yb_2O_3)

(JCPDS 22-0612), respectively. On the other hand, samples calcined at 750 °C exhibited, in all cases, lines corresponding to the MgAlO mixed oxide phase with the periclase-like structure (JCPDS-ICDD 4-0829) and lines corresponding to CeO_2 (JCPDS 75-0076), Sm_2O_3 (JCPDS 15-0813), Dy_2O_3 (JCPDS 22-0612) and Yb_2O_3 (JCPDS 41-1106) phases for Ce-, Sm-, Dy- and Yb–Mg–Al–O mixed oxides, respectively. We note that XRD patterns of the samples after the catalytic test remained practically unchanged.

The chemical compositions of the samples reported in Table 1 show that the rare-earth content was slightly higher than the nominal value and the Mg/Al atomic ratio varied between 2.9 for Ce–Mg–Al–O and 3.9 for Yb–Mg–Al–O.

The specific surface areas of the catalysts were high, in the range 102–160 $m^2\ g^{-1}$. They are also reported in Table 1. All the catalysts displayed type IV nitrogen adsorption/desorption isotherms, according to IUPAC classification, with a hysteresis loop characteristic of mesoporous materials [18] with a broad distribution of sizes. After the catalytic test, the specific surface areas of the catalysts remained practically the same.

The TG-DTG curves of YbMgAl-LDH precursor and of the corresponding oxide, Yb–Mg–Al–O, are presented in Fig. 3. The first weight loss in the TG-DTG curves of the HDL precursor (Fig. 3a) is due to the elimination of loosely bound water and interlayer water molecules. The second weight loss is ascribed to the removal of hydroxyl groups in the metal hydroxide layers. The sample exhibited a net weight loss of 43% up to 900 °C, with the second weight loss being larger than the first one. This is in accord with literature data for hydrotalcite-like materials [19–21]. In the case of the calcined oxide, the TG curve decreased continuously up to 500 °C but the DTG profile presented two well-defined signals at 90 and 185 °C and a broad signal in the range 250–500 °C (Fig. 3b). The total weight loss for the calcined sample was smaller, namely 15%. This may be due to the adsorption of water and carbon dioxide from the environmental air at the oxide surface and suggests that the catalyst must be activated in the reactor before the catalytic test at temperatures higher than 500 °C for cleaning its surface.

The basicity of the catalysts was determined by temperature-programmed desorption of CO_2 (CO_2-TPD), the profiles obtained being shown in Fig. 4. These profiles were deconvoluted in three CO_2 desorption peaks, having the maximum in the range of 175–185, 225–250 and 300–340 °C demonstrating that they have basic sites of different strengths: weak, moderate and strong. The total basicity was calculated according to the desorbed amount of CO_2

Table 1 Physico-chemical characteristics of the catalysts

Catalyst	SSA[a] (m^2 g^{-1})	Chemical composition (% at.) by EDX[b]			Ln/(Ln + Mg + Al) atomic ratio	Mg/Al atomic ratio	Total basicity (mmol CO_2/g)	Total H_2 consumption (mol H_2/mol Ln)
		Ln	Mg	Al				
Ce–Mg–Al–O	157	1.7	21.1	7.2	5.6	2.9	1.63	0.13
Sm–Mg–Al–O	160	1.8	26.0	7.1	5.2	3.6	2.18	0.12
Dy–Mg–Al–O	102	1.5	21.3	7.0	5.1	3.1	2.52	0.18
Yb–Mg–Al–O	142	1.9	25.3	6.5	5.6	3.9	1.96	0.19

[a] Specific surface area

[b] Oxygen in balance

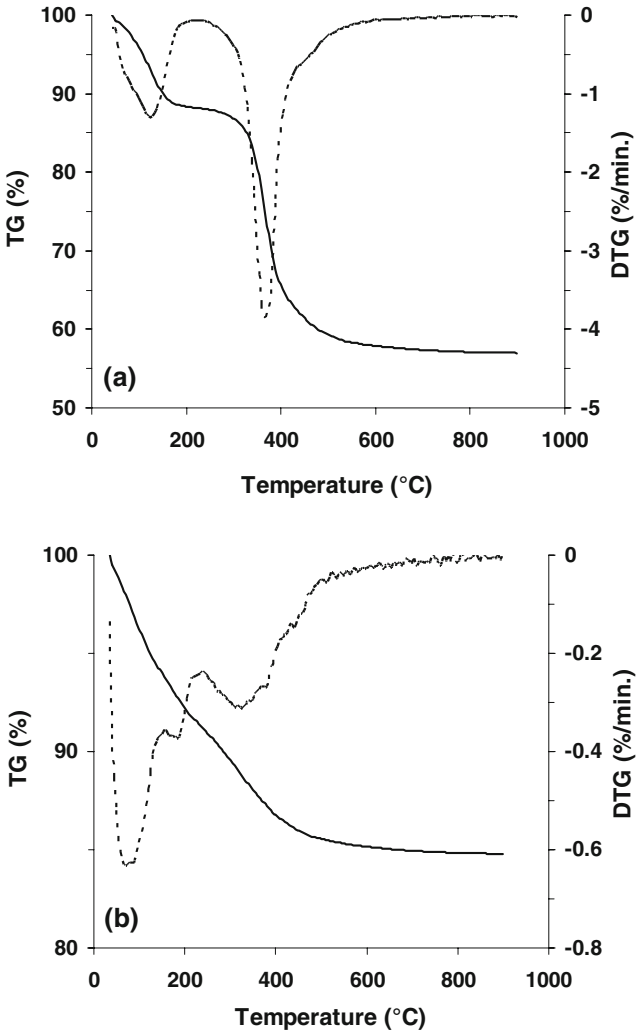

Fig. 3 TG-DTG profiles of uncalcined YbMgAl-LDH precursor (**a**) and of the resulting Yb–Mg–Al–O mixed oxide (**b**)

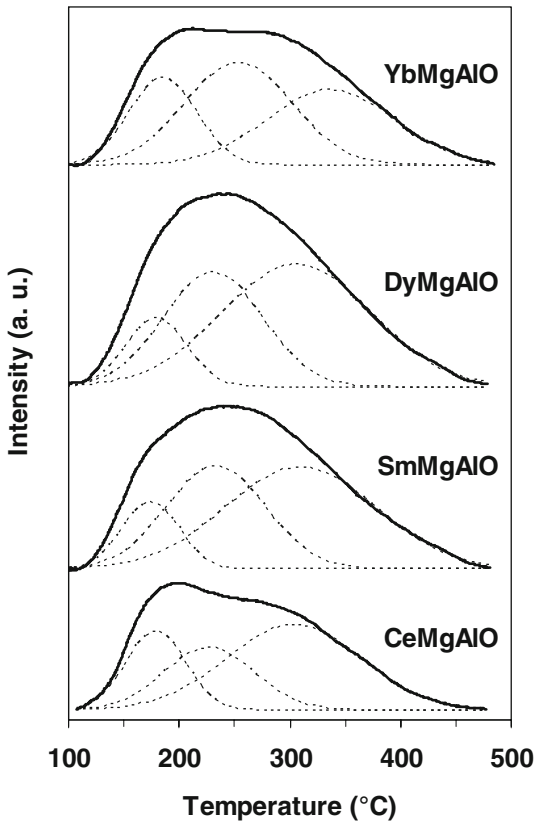

Fig. 4 CO_2-TPD profiles of the Ln–Mg–Al–O mixed oxide catalysts

and summarized in Table 1. The total basicity followed the order: Dy > Sm > Yb > Ce.

TPR experiments have been carried out over all the mixed oxide samples prepared in order to study the redox properties of the catalysts. The TPR patterns of the catalysts are presented in Fig. 5. All the samples displayed at high temperatures a large not well-defined pattern which was decomposed in two reduction peaks. These peaks must correspond to the reduction of the tetravalent cation (Ce) according to the equation: $Ce^{4+} \rightarrow Ce^{3+}$, and to the reduction of trivalent Ln^{3+} cations according to the equation: $Ln^{3+} \rightarrow Ln^{2+}$. The low-temperature peak could be attributed to the reduction of the rare-earth cationic species from the rare-earth oxide clusters, and the high-temperature peak, attributed to the reduction of rare-earth cationic species in the large crystalline rare-earth oxide particles. We note that for Sm–Mg–Al–O sample a well-defined low intensity peak was also observed before the large pattern. It

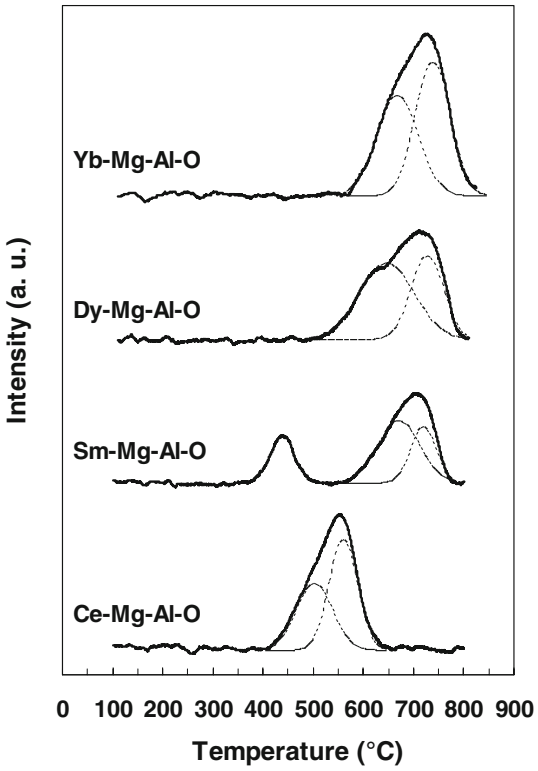

Fig. 5 H_2-TPR profiles for Ln–Mg–Al–O samples

could be due to the reduction of the easily reducible samarium species from highly dispersed samarium oxide. These results suggest a non-uniform dispersion of the rare-earth oxide in the Mg–Al mixed oxide matrix. Assuming the reduction according to the equations above, 0.5 moles of H_2 per mol of Ln would be necessary. The data from Table 1 show that much lower quantities of H_2 were experimentally consumed indicating that only a partial reduction of rare-earth cations occurred.

3.2 Catalytic Oxidative Dehydrogenation

Firstly blank tests have been done without a catalyst, the catalyst bed being replaced with quartz. Figure 6a shows that the non-catalytic oxidative conversion of propane is not significant in our testing conditions, at least at temperatures below 600 °C, confirming that the contribution of the homogeneous reaction was negligible.

The conversion of propane and the product selectivities as a function of reaction temperature for the reaction with propane–air mixtures at a total VHSV of 9,000 h^{-1} and a propane-to-oxygen molar ratio equal to 2, over the tested catalysts are depicted in Fig. 6. For all the catalysts the conversion increased with increasing the reaction temperature while the propene selectivity decreased to the benefit of CO_x for Ce-based system and of cracking products for the other systems. We note that the Yb-based system was not

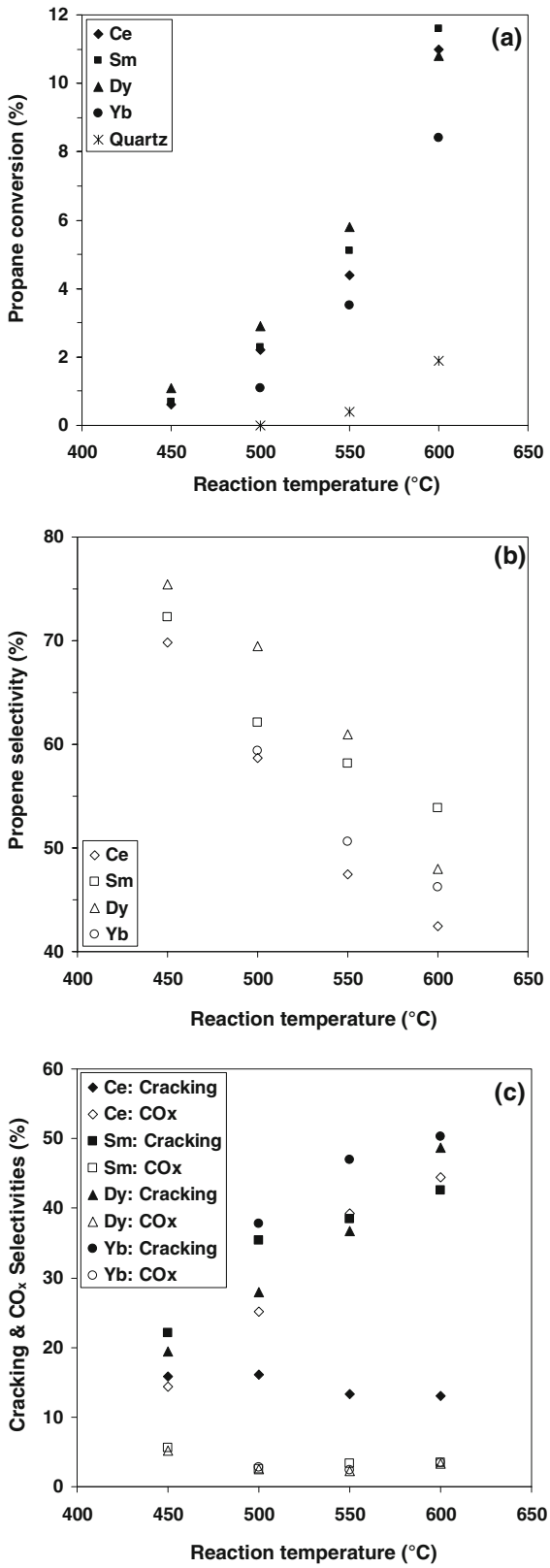

Fig. 6 Propane conversion (**a**), propene selectivity (**b**) and cracking and CO_x selectivities (**c**) as a function of reaction temperature over Ln–Mg–Al–O mixed oxide catalysts (propane-to-oxygen molar ratio = 2, total VHSV = 9,000 h^{-1})

active at temperatures lower than 500 °C. For the reaction at 500 °C the catalytic activity followed the order: Dy > Sm ≥ Ce > Yb. The differences in conversions indicate the influence of the metallic properties on the rate-determining hydrogen abstraction by the catalysts [14]. In the case of Ce–Mg–Al–O system, the sum of the selectivities of CO_x and CH_4 was not equal to that of ethylene, as was the case with the other systems, but much higher within all the range of temperatures studied. This suggests that for Ce-based system, total oxidation products (CO_x) were formed not only from C1 species resulting from the cracking of propane, but also by the direct oxidation of propane or by further oxidation of propene. This was not the case for Sm-, Dy and Yb–Mg–Al–O catalysts.

The apparent activation energies (E_{act}) corresponding to the propane transformation on the different catalysts have been calculated (Table 2) from the Arrhenius plots presented in Fig. 7. The activation energies increased following the order Dy < Sm ≤ Ce < Yb, in line with the observed variation of the catalytic activity. On the other hand, the values obtained for the activation energies fall within the usual range measured for propane oxidative dehydrogenation over oxide-based catalysts [22, 23].

Table 2 Apparent activation energies corresponding to the propane transformation on the Ln–Mg–Al–O catalysts

Catalyst	E_{act} (kcal mol^{-1})
Ce–Mg–Al–O	23.7
Sm–Mg–Al–O	23.2
Dy–Mg–Al–O	19.0
Yb–Mg–Al–O	27.3

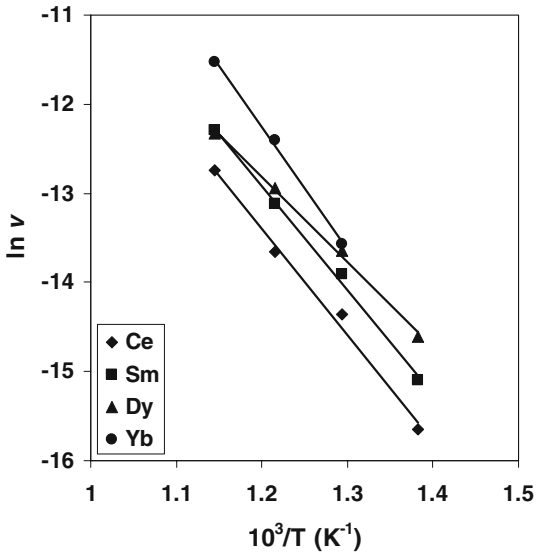

Fig. 7 Arrhenius plots for the propane conversion on the tested catalysts

The effect of the conversion on the selectivities has been studied for the reactions over all Ln–Mg–Al–O catalysts at 550 °C and a propane-to-oxygen molar ratio equal to 2, by varying the VHSV in the range 3,000–12,000 h^{-1} (Fig. 8).

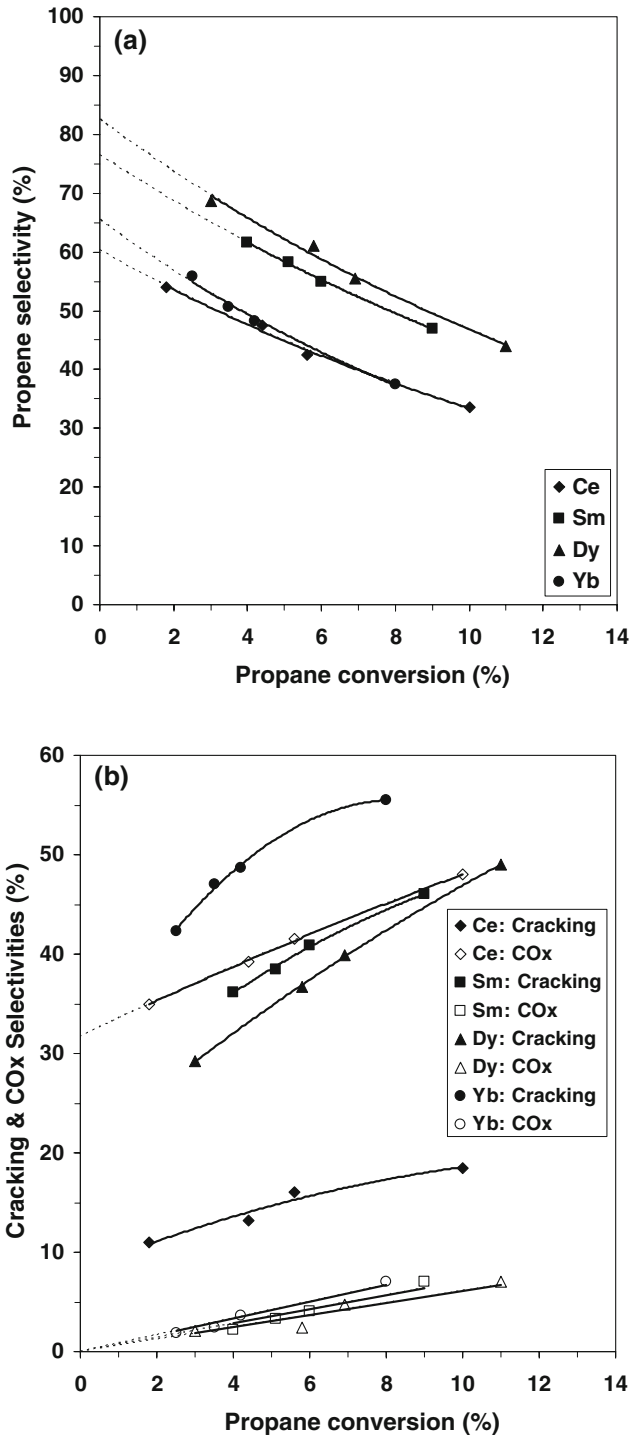

Fig. 8 Effect of conversion on the propene selectivity (**a**) and cracking and CO_x selectivities (**b**) in the oxidative dehydrogenation of propane over Ln–Mg–Al–O mixed oxide catalysts at 550 °C (propane-to-oxygen molar ratio = 2)

As expected, the selectivity to propene decreased in all cases with increasing conversion. The extrapolation to zero conversion results, for the reaction over Ce-based system, in non-zero selectivity for carbon oxides and cracking products indicating that they are also primary products formed simultaneously with propene. For the reaction over other Ln-based systems studied, the extrapolation to zero conversion results in zero carbon oxides selectivity and non-zero selectivity for cracking products showing that only the latter are also primary products, carbon oxides being not in this case. These results confirm that, among the catalysts studied, the parallel reaction of propane leading to carbon oxides is specific only for Ce-based system.

On the other hand, the conversion-selectivity curves clearly showed that the oxidative dehydrogenation selectivity followed the order: Dy > Sm > Yb > Ce. The changes in the selectivities on the studied catalysts indicate the effect of Ln properties on the selectivity.

The effect of the propane-to-air molar ratio on the oxidative dehydrogenation of propane over Dy-based catalyst is presented in Fig. 9. The propane conversion strongly decreased when the propane-to-oxygen molar ratio increased from 1 to 4. At the same time the selectivity to propene increased at the expense of cracking products and carbon oxides. These results could be explained by the decrease of the available oxygen related to the increase in the propane-to-oxygen ratio. Moreover, the observed decrease of the selectivity for cracking products can be explained taking into consideration that when the propane-to-oxygen molar ratio was increased keeping the total VHSV constant, the partial pressure of propane in the reaction mixture increased, cracking being thus disadvantaged.

A linear correlation between the catalyst CO_2-TPD basicity and the propene selectivity was observed as shown in Fig. 10 both for the reaction at 500 and 550 °C. The direct relationship found between surface basicity and propene selectivity can be accounted for by the electron-donating character of the olefinic species and the consequent easier desorption from a more basic surface, thus preventing further overoxidation into carbon oxides. Interestingly, the most selective catalysts proved the most active as well (Fig. 6).

We note that the Mg–Al mixed oxide-supported rare-earth oxides studied in this work exhibit better performance in terms of selectivity to propene than the γ-Al_2O_3-supported rare-earth oxides in Ref. [14], confirming the expected effect of magnesium.

Finally, we note that no correlation between the H_2-TPR reducibility of the rare-earth cation and the catalytic performances was observed, suggesting that the surface-adsorbed oxygen but not lattice oxygen species are involved in the reaction. A similar result was obtained by Al-Zahrani et al. [14] for γ-Al_2O_3-supported rare-earth oxide catalysts by estimating the lattice oxygen reactivity from the reduction potential of the cation.

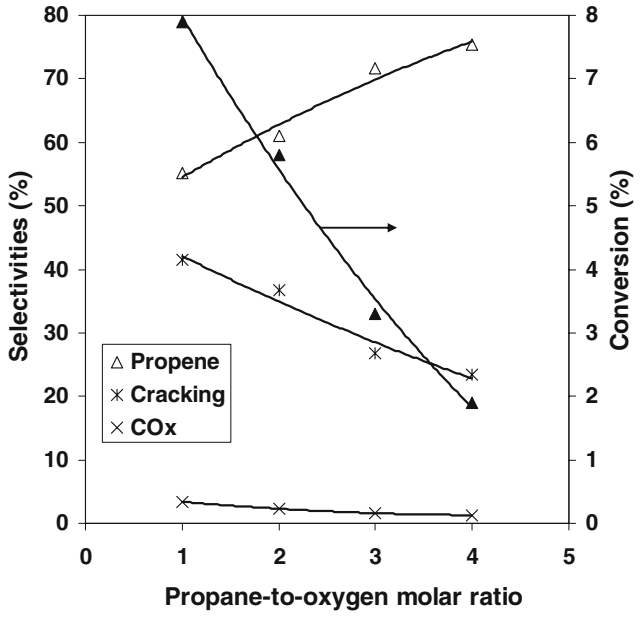

Fig. 9 Effect of propane-to-oxygen molar ratio on the oxidative dehydrogenation of propane over Dy–Mg–Al–O catalyst at 550 °C (total VHSV = 9,000 h^{-1})

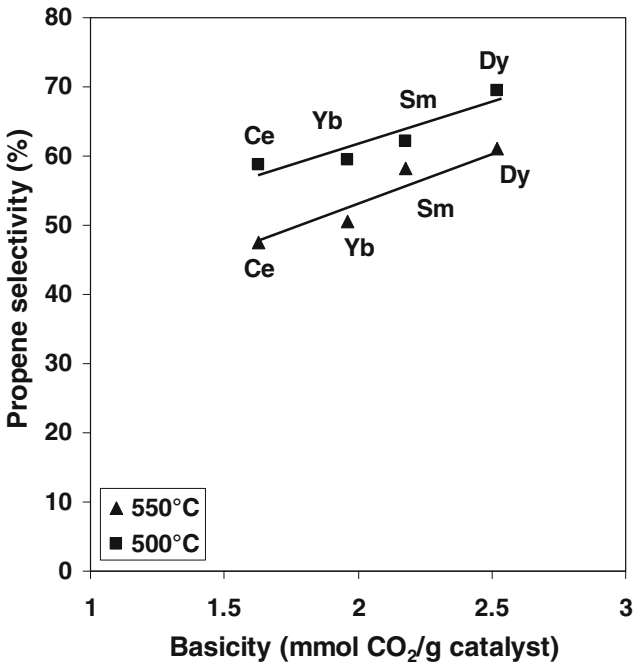

Fig. 10 Propene selectivity versus the catalyst basicity for the reaction at 500 and 550 °C over the studied catalysts

4 Conclusions

The properties of basic Ln–Mg–Al mixed oxides catalysts for the ODH of propane have been investigated in the temperature range 450–600 °C. For all the catalysts the conversion increased with increasing the reaction temperature while the propene selectivity decreased. The best yields in propene were obtained with Dy- and Sm–Mg–Al–O systems, Dy-based catalyst being the most selective one. Increasing the propane-to-oxygen molar ratio from 1 to 4 for Dy-based catalyst, the propane conversion decreased from 8 to 2% but the propene selectivity increased from 55 to 75% at the expense of cracking products and carbon oxides. A linear correlation between the catalyst basicity and the propene selectivity was observed. On the other hand, no correlation between the H_2-TPR reducibility of the rare-earth cation and the catalytic performances was observed.

Acknowledgment This research was supported by the Romanian National University Research Council (CNCSIS) under the project "IDEI" No. 1906/2009.

References

1. D'Ippolito SA, Bañares MA, Garcia Fierro JL, Pieck CL (2008) Catal Lett 122:252
2. Karakoulia SA, Triantafyllidis KS, Lemonidou AA (2008) Micro Meso Mater 110:157
3. Sugiyama S, Osaka T, Hirata Y, Sotowa KI (2006) Appl Catal A 312:52
4. Dźwigaj S, Gressel I, Grzybowska B, Samson K (2006) Catal Today 114:237
5. Koc SN, Gurdag G, Geissler S, Guraya M, Orbay M, Muhler M (2005) J Mol Catal A 225:197
6. Heracleous E, Machli M, Lemonidou AA, Vasalos IA (2005) J Mol Catal A 232:29
7. Bañares MA, Khatib SJ (2004) Catal Today 96:251
8. Davies T, Taylor SH (2004) J Mol Catal A 220:77
9. Zhaorigetu B, Li W, Xu H, Kieffer R (2004) Catal Lett 94:125
10. Wu Y, He Y, Chen T, Weng W, Wan H (2006) Appl Surf Sci 252:5220
11. He Y, Wu Y, Chen T, Weng W, Wan H (2006) Catal Commun 7:268
12. Trionfetti C, Babich IV, Seshan K, Lefferts L (2006) Appl Catal A 310:105
13. Jibril BY (2005) Ind Eng Chem Res 44:702
14. Al-Zahrani SM, Jibril BY, Abasaeed AE (2003) Catal Lett 85:57
15. Buyevskaya OV, Wolf D, Baerns M (2000) Catal Today 62:91
16. Zhang W, Zhou X, Tang D, Wan H, Tsai K (1994) Catal Lett 23:103
17. Rives V, Ulibarri MA (1999) Coord Chem Rev 181:61
18. IUPAC Reporting physisorption data for gas/solid system (1985) Pure Appl Chem 57:603
19. Das J, Das D, Parida KM (2006) J Coll Int Sci 301:569
20. Tichit D, Das N, Coq B, Durand R (2002) Chem Mater 14:1530
21. Parida KM, Das J (2000) J Mol Catal A Chem 151:185
22. Mattos ARJM, da Silva San Gil RA, Rocco MLM, Eon J-G (2002) J Mol Catal A 178:229
23. Male JL, Niessen HG, Bell AT, Tilley TD (2000) J Catal 194:431